

Supplement of Earth Syst. Dynam., 7, 419–439, 2016
<http://www.earth-syst-dynam.net/7/419/2016/>
doi:10.5194/esd-7-419-2016-supplement
© Author(s) 2016. CC Attribution 3.0 License.



Supplement of

Are there multiple scaling regimes in Holocene temperature records?

T. Nilsen et al.

Correspondence to: Tine Nilsen (tine.nilsen@uit.no)

The copyright of individual parts of the supplement might differ from the CC-BY 3.0 licence.

S1 The Lomb-Scargle periodogram as an alternative spectral estimator for the unevenly sampled ice core data

While the standard periodogram is based on Fourier analysis (Schuster, 1898), the LSP is based on a least-squares fit of sinusoids to the data. We use the R package *lomb*, and the power is normalized by multiplying by σ^2/N , where σ^2 is the variance. For time series of N data points $Y_j = Y(t_j)$ collected at times t_j where $j = 1, 2, \dots, N$, with mean value \bar{Y} , the

5 Lomb-Scargle periodogram is defined as,

$$S_N(\omega) = \frac{1}{2\sigma^2} \left\{ \frac{\left[\sum_j (Y_j - \bar{Y}) \cos \omega(t_j - \tau) \right]^2}{\sum_j \cos^2 \omega(t_j - \tau)} + \frac{\left[\sum_j (Y_j - \bar{Y}) \sin \omega(t_j - \tau) \right]^2}{\sum_j \sin^2 \omega(t_j - \tau)} \right\}, \quad (1)$$

with

$$\tau = \left(\frac{1}{2\omega} \right) \tan^{-1} \left[\frac{\sum_j \sin 2\omega t_j}{\sum_j \cos 2\omega t_j} \right] \quad (2)$$

10

S1.1 Test of the Lomb-Scargle periodogram - surrogate data mimicking ice core proxy data

The Lomb-Scargle periodogram (LSP) was originally designed to detect a periodic signal hidden in noise, and has been applied to periodic data with random missing values such as astronomical observations (Lomb, 1976; Scargle, 1982), biological rhythms (Ruf, 1999; Van Dongen et al., 1999), and heart-rate signals (Laguna et al., 1998). In the proxy-based climatic time series we don't expect perfect periodicities, and data points are not randomly missing. The sampling interval rather increases systematically as one goes backward in time. It is therefore not a priori obvious that this method can give confident estimates of the scaling exponent for the ice core time series. Pelletier (1998) used the Lomb periodogram to estimate the scaling exponent for temperature inferred from the Vostok ice core, but did not discuss the sensitivity of the method.

15

We perform such a test on ensembles of synthetic fGn's and fBm's, respectively. For each realization in the ensemble, the scaling exponent is estimated from the LSP. The mean exponent value as well as the error based on the 2.5% and 97.5% quantiles are estimated. The LSP gives the same results as the ordinary periodogram when the sampling is even. The method is tested by removing data points from the synthetic data sets and repeat the estimation for each realization. Data is removed in such a manner that the sampling intervals become identical to those we find in ice core data. We have chosen a section of the low-resolution GRIP $\delta^{18}\text{O}$ time series covering the Holocene, and another one from the last glacial period as the basis for this test (see the main article, Sect. 4.3 for data description). The test is carried out by first generating surrogate data sets where the time step is chosen to be the least time step in the observed record. The surrogate time series is then interpolated, and we sample this interpolation function at the times known from the ice core time series. The "resampled" time series has the same number of data points as the GRIP Holocene/last glacial period time series, and β is estimated in the range $\frac{1}{20} - \frac{1}{333} \text{ yr}^{-1}$ for the Holocene, and $\frac{1}{200} - \frac{1}{3333} \text{ yr}^{-1}$ for the last glacial period.

25

Fig. S1 shows the result when surrogate data are sampled like the low-resolution GRIP Holocene (Fig. S1a,c) and low-resolution GRIP last glacial period (Fig. S1b,d). In Fig. S1a,b, observe a slight negative bias for β , caused by the LSP. The difference between the upper and lower panels is due to an important detail when generating our surrogate data. In the top panel, our surrogate data are sampled at irregular time steps, but as point measurements. In reality, the given values of stable isotopes from ice cores are generally averages over the time period covered by the sliced equal-length samples. The real proxy values will therefore exhibit less variability than if they were instantaneous measurements of the true temperature. This smoothing effect will increase as one goes back in time due to compression of the core. The smoothing effect constitutes a positive bias that works in the opposite direction of the negative bias introduced by the LSP. Taking this into account we have created surrogate data (Fig. S1c,d) that resembles proxy data to a larger degree than in the topmost panel.

35

Because the least time step between values is different in the GRIP Holocene and last glacial period, the lengths of the synthetic data sets are also different. This leads to different error bars for the estimates. From Fig. S1c,d we observe that the estimated β

40

is close to the true β , except for true β slightly greater than unity. The negative bias observed for β slightly higher than unity is expected, and is present also in the standard periodogram. It is due to a spectral feature arising when the (continuous-time) fBm is sampled at discrete times: the spectrum flattens when the Nyquist frequency is approached for β slightly above unity, and leads to an underestimation of β if these frequencies are used in the fitting of a straight line in the log-log plot. Bias and errors are similar to the standard periodogram and shows that the LSP is a very useful substitution for the periodogram for these data records.

Another test of the LSP is also presented for data with constant sampling intervals where data points are missing randomly. This test is more general, since such data are not dealt with in the paper.

S1.2 Test of the Lomb-Scargle periodogram - random removal of data

10 Systematically we remove 25%, 50% and 75% of the data points from Monte Carlo ensembles of synthetic fGn's and fBm's. Fig. S2 shows the estimated scaling exponent vs. the true exponent for the even sampling case, and when 25%, 50% and 75% of the data points are removed.

In Fig. S2b,c,d we observe that when more data is removed, β is gradually more underestimated. This can be explained from Fig. S3 which shows increasing power at the high frequencies when data is removed. The LSP method fits sinusoids to the data on different frequencies, and the low frequency variability is mostly unaffected by the removal of data. For the high frequencies on the other hand, removal of data allows good fit of sinusoids with larger amplitude.

Fig. S2 demonstrates that serious underestimation of β can result from applying the LSP to time series with randomly missing data, if the true β is larger than unity.

S1.3 Spectral analysis of ice core data using the Lomb-Scargle periodogram

20 As a supplement to the spectral analysis in the main article, the same data are here analysed using the LSP. The resulting spectra and scale-break features are similar as the results when interpolation and the standard periodogram are used.

For the GRIP high resolution ice core, fig S4 shows the $\delta^{18}\text{O}$ time series and corresponding LSP for the Holocene. The topmost figures are for the full Holocene time period, where $\beta \approx 0.3$ on time scales up to 10^3 yr. The lower panel is for the most recent 7.5 kyr of the Holocene. The spectrum is essentially flat for the same time period.

25 Fig S5 shows the $\delta^{18}\text{O}$ time series for the last glacial period of the high-resolution GRIP ice core, and the LSP for the same time period. $\beta \approx 1.4$ on time scales longer than 10^2 yr and shorter than 10^4 yr.

Fig S6 shows the $\delta^{18}\text{O}$ time series for the past 85 kyr of the high-resolution GRIP ice core, and the LSP for the same time period. The estimated value of β is the same as in fig S5 on the same time scales.

30 For the EPICA ice core, fig S7 shows the δD time series and corresponding LSP for the Holocene. $\beta \approx 0.2$ on time scales up to millenia. For the last glacial period of EPICA, fig S8 shows the δD time series and corresponding LSP. $\beta \approx 1.8$ on time scales longer than 10^3 yr and shorter than 10^4 yr.

S2 Analysis of additional four deep ice core time series

To support our results in the main article, we present here the analyses of additional four deep ice cores from Greenland and Antarctica. The Greenland ice cores are GISP2, (Grootes et al., 1993; Grootes and Stuiver, 1997) and NGRIP, (North Greenland Ice-Core project (NGRIP) members, 2004; Andersen et al., 2006; Vinther et al., 2006; Rasmussen et al., 2006; Svensson et al., 2008; Wolff et al., 2010). From Antarctica we include the Taylor dome ice core, (Steig et al., 2000), and Vostok, (Lorius et al., 1985; Jouzel et al., 1987, 1993). We include only results using interpolation and the standard periodogram, and not the LSP.

S2.1 Results from the GISP2 and NGRIP ice cores

40 Figure S9 shows (a) the $\delta^{18}\text{O}$ time series of the Holocene part of the GISP2 ice core, and (b) the periodogram for the same time series. No scale break is detected on centennial time scales, and the estimated $\beta \approx 0.2$. (c) shows the $\delta^{18}\text{O}$ time series of

the Holocene part of the NGRIP ice core, and (d) the periodogram for the same time series, where we estimate $\beta \approx 0.35$ and no scale break at centennial time scales.

Figure S10 displays (a) The $\delta^{18}\text{O}$ time series for the GISP2 ice core from the last glacial period, and (b) the periodogram for the same time series, where we estimate $\beta \approx 1.1$. (c) shows the $\delta^{18}\text{O}$ time series for the NGRIP ice core from the last glacial period, and (d) the periodogram for the same time series with estimated $\beta \approx 1.4$.

S2.2 Results from the Taylor and Vostok ice core

Figure S11 shows (a) the Holocene time series of the Taylor ice core, and (b) the periodogram for the same time series where we estimate $\beta \approx 0.2$ for time scales shorter than 10^3 yr. (c) shows the Holocene time series from the Vostok ice core, and (d) the periodogram for the same time series. Due to the poor temporal resolution of the Vostok paleotemperature time series, the periodogram has few data points and the uncertainties are therefore larger for this time series than others studied. Further, the periodogram is affected by the smoothing of the δD time series. This is observed as an abrupt decrease in power at the highest frequencies, and a linear fit should be avoided in this area. We obtain $\beta \approx 0.1$ from the periodogram, but note that this time series can not be used to infer the scaling at centennial time scales.

Figure S12 shows (a) The $\delta^{18}\text{O}$ time series for the Taylor ice core from the last glacial period, and (b) the periodogram for the same time period where we estimate $\beta \approx 1.9$. (c) shows the δD time series for the Vostok ice core from the last glacial period, and (d) the periodogram for the same time period with estimated $\beta \approx 1.7$.

References

- Andersen, K. K., Svensson, A., Johnsen, S. J., Rasmussen, S. O., Bigler, M., Röthlisberger, R., Ruth, U., Siggaard-Andersen, M.-L., Steffensen, J. P., Dahl-Jensen, D., Vinther, B. M., and Clausen, H. B.: The Greenland Ice Core Chronology 2005, 15-42 ka. Part 1: constructing the time scale, *Quaternary Sci. Rev.*, 25, 3246–3257, Shackleton special issue 24, 2006.
- Grootes, P. M. and Stuiver, M.: Oxygen 18/16 variability in Greenland snow and ice with 10^3 to 10^5 -year time resolution, *Journal of Geophysical Research: Oceans*, 102, 26 455–26 470, doi:10.1029/97JC00880, 1997.
- Grootes, P. M., Stuiver, M., White, J. W. C., Johnsen, S., and Jouzel, J.: Comparison of oxygen isotope records from the GISP2 and GRIP Greenland ice cores, *Nature*, 366, 552–554, doi:10.1038/366552a0, 1993.
- Jouzel, J., Lorius, C., Petit, J. R., Genthon, C., Barkov, N. I., Kotlyakov, V. M., and Petrov, V. M.: Vostok ice core: a continuous isotope temperature record over the last climatic cycle (160,000 years), *Nature*, 329, 403–408, doi:10.1038/329403a0, 1987.
- Jouzel, J., Barkov, N. I., Barnola, J. M., Bender, M., Chappellaz, J., Genthon, C., Kotlyakov, V. M., Lipenkov, V., Lorius, C., Petit, J. R., Raynaud, D., Raisbeck, G., Ritz, C., Sowers, T., Stievenard, M., Yiou, F., and Yiou, P.: Extending the Vostok ice-core record of palaeoclimate to the penultimate glacial period, *Nature*, 364, 407–412, doi:10.1038/364407a0, 1993.
- Laguna, P., Moody, G. B., and Mark, R. G.: Power Spectral Density of Unevenly Sampled Data by Least-Square Analysis: Performance and Application to Heart Rate Signals, *IEEE T. BIO-MED. ENG.*, 45, 698–715, doi:10.1109/10.678605, 1998.
- Lomb, N. R.: Least-squares frequency analysis of unequally spaced data, *Astrophys. Space Sci.*, 39, 447–462, 1976.
- Lorius, C., Jouzel, J., Ritz, C., Merlivat, L., Barkov, N. I., Korotkevich, Y. S., and Kotlyakov, V. M.: A 150,000-year climatic record from Antarctic ice, *Nature*, 316, 591–596, doi:10.1038/316591a0, 1985.
- North Greenland Ice-Core project (NGRIP) members: High-resolution record of Northern Hemisphere climate extending into the last interglacial period, *Nature*, 431, 147–151, doi:10.1038/nature02805, 2004.
- Pelletier, J. D.: The power spectral density of atmospheric temperature from time scales of 10^{-2} to 10^6 yr., *Earth and Planetary Science Letters*, 158, 157–164, doi:10.1016/S0012-821X(98)00051-X, 1998.
- Rasmussen, S. O., Andersen, K. K., Svensson, A. M., Steffensen, J. P., Vinther, B. M., Clausen, H. B., Siggaard-Andersen, M.-L., Johnsen, S. J., Larsen, L. B., Dahl-Jensen, D., Bigler, M., Röthlisberger, R., Fischer, H., Goto-Azuma, K., Hansson, M. E., and Ruth, U.: A new Greenland ice core chronology for the last glacial termination, *J. Geophys. Res-Atmos.*, 111, doi:10.1029/2005JD006079, 2006.
- Ruf, T.: The Lomb-Scargle Periodogram in Biological Rhythm Research: Analysis of Incomplete and Unequally Spaced Time-Series, *Biol. Rhythm Res.*, 30, 178–201, doi:10.1076/brhm.30.2.178.1422, 1999.
- Scargle, J. D.: Studies in astronomical time series analysis. II. Statistical aspects of spectral analysis of unevenly sampled data, *Astrophys. J.*, 263, 835–853, doi:10.1086/160554, 1982.
- Schuster, A.: On the investigation of hidden periodicities with application to a supposed 26 day period of meteorological phenomena., *Terrestrial Magnetism*, 3, 13–41, doi:10.1029/TM003i001p00013, 1898.
- Steig, E. J., Morse, D. L., Waddington, E. D., Stuiver, M., Grootes, P. M., Mayewski, P. A., Twickler, M. S., and Whitlow, S. I.: Wisconsinan and Holocene Climate History from an Ice Core at Taylor Dome, Western Ross Embayment, Antarctica, *Geogr. Ann. A.*, 82, 213–235, 2000.
- Svensson, A., Andersen, K., Bigler, M., Clausen, H., Dahl-Jensen, D., Davies, S., Johnsen, S., Muscheler, R., Rasmussen, S., Röthlisberger, R., Seierstad, I., Steffensen, J., and Vinther, B.: A 60 000 year Greenland stratigraphic ice core chronology, *Clim. Past*, 4, 47–57, doi:10.5194/cp-4-47-2008, 2008.
- Van Dongen, H. P. A., Olofson, E., VanHartevelt, J. H., and Kruyt, E. W.: Searching for Biological Rhythms: Peak Detection in the Periodogram of Unequally Spaced Data, *J. Biol. Rhythm*, 14, 617–620, doi:10.1177/074873099129000984, 1999.
- Vinther, B. M., Clausen, H. B., Johnsen, S. J., Rasmussen, S. O., Andersen, K. K., Buchardt, S. L., Dahl-Jensen, D., Seierstad, I. K., Siggaard-Andersen, M.-L., Steffensen, J. P., Svensson, A., Olsen, J., and Heinemeier, J.: A synchronized dating of three Greenland ice cores throughout the Holocene, *J. Geophys. Res-Atmos.*, 111, D13 102, doi:10.1029/2005JD006921, 2006.
- Wolff, E. W., Chappellaz, J., Blunier, T., Rasmussen, S., and Svensson, A.: Millennial-scale variability during the last glacial: The ice core record, *Quaternary Sci. Rev.*, 29, 2828–2838, doi:10.1016/j.quascirev.2009.10.013, 2010.

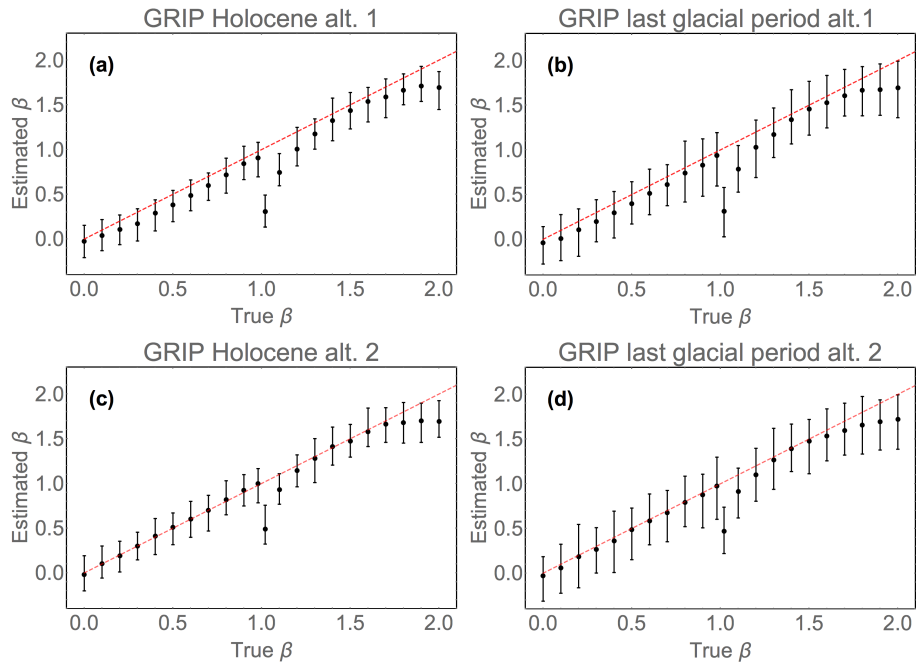


Figure S1. Value of estimated β vs. true β from 100 realizations of synthetic LRM processes. (a) Temporal sampling equal to a point measurement from the low-resolution GRIP Holocene time series. (b) Temporal sampling equal to a point measurement of the low-resolution GRIP last glacial time series. (c,d) As in a,b, respectively, but with data points corresponding to temporal averages.

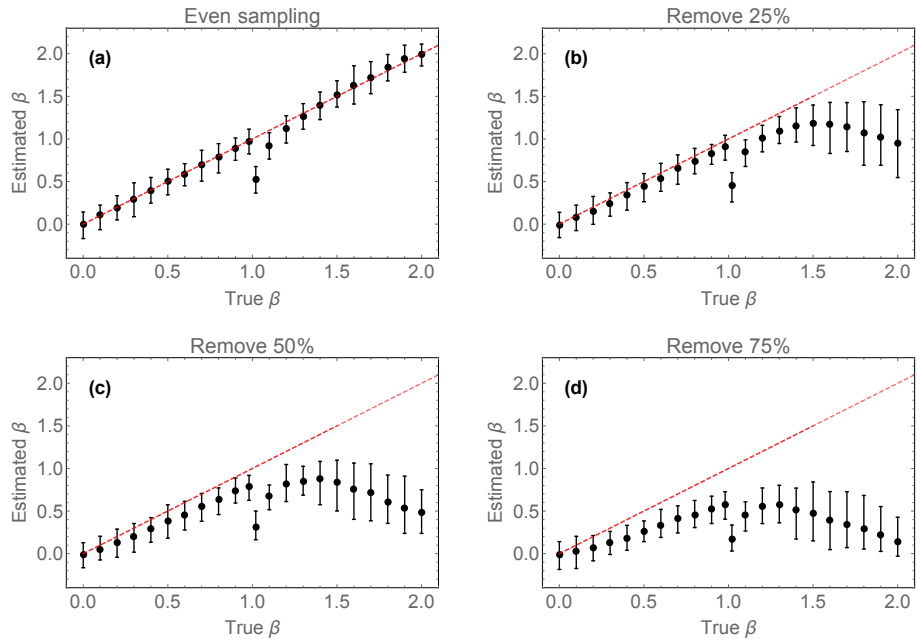


Figure S2. Value of estimated β vs. true β from 100 realizations of synthetic data. (a) Evenly sampled time series, 12576 data points. (b) 25% removed. (c) 50% removed. (d) 75% removed.

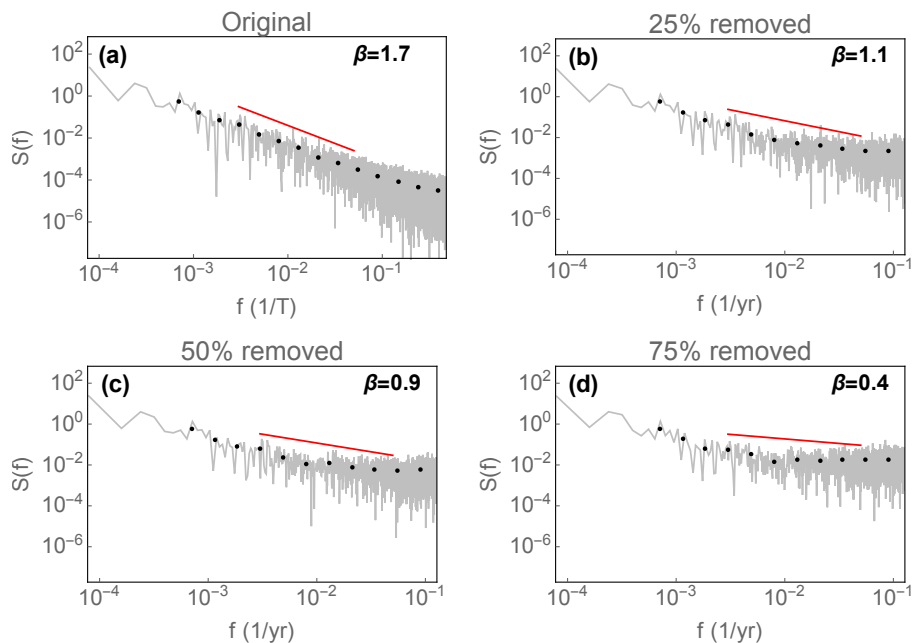


Figure S3. LSP for an fBm with $\beta=1.6$, with 12 576 data points. (a) Original time series. (b) 25% removed. (c) 50% removed. (d) 75% removed.

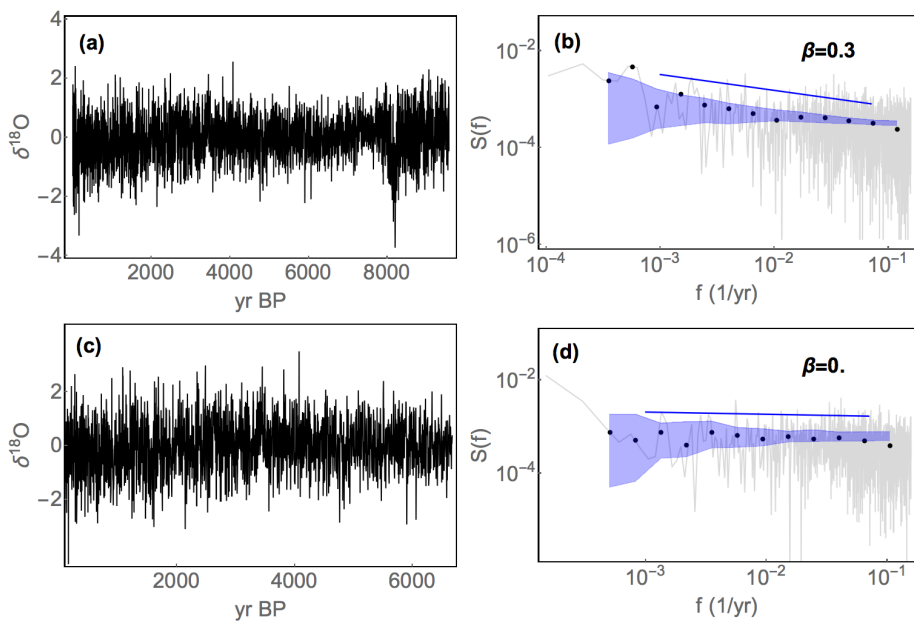


Figure S4. (a): $\delta^{18}\text{O}$ anomalies from the Holocene part of the high-resolution GRIP ice core. (b): Lomb-Scargle periodogram. The raw LSP is shown in gray, the log-binned version by black dots. β is estimated from the log-binned LSP in the region marked by the blue line. The confidence range is shown by the blue, shaded area, estimated from a Monte Carlo ensemble of synthetic fGns with the estimated value of β and variance from the log-binned LSP. (c) Same figure as in (a) except the oldest section has been removed. (d) Lomb-Scargle periodogram for the time series in (c).

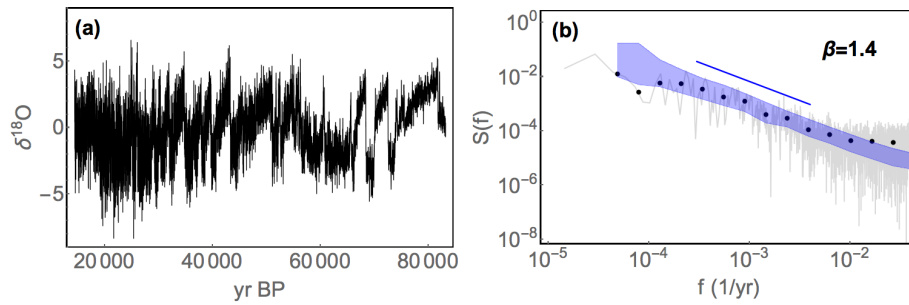


Figure S5. (a): $\delta^{18}\text{O}$ anomalies from the last glacial period of the high-resolution GRIP ice core. (b): Lomb-Scargle periodogram.

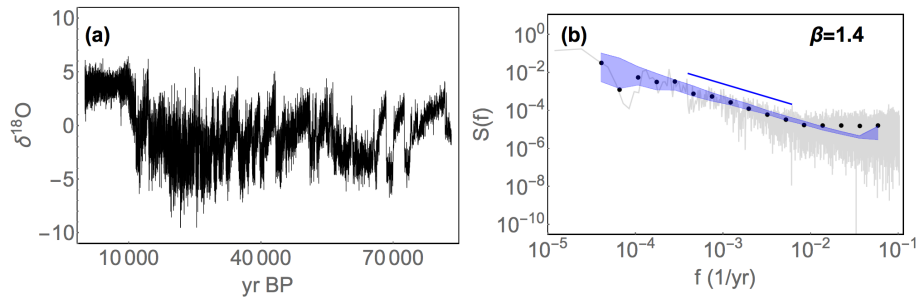


Figure S6. (a): $\delta^{18}\text{O}$ anomalies from the past 85 kyr of the high-resolution GRIP ice core. (b): Lomb-Scargle periodogram

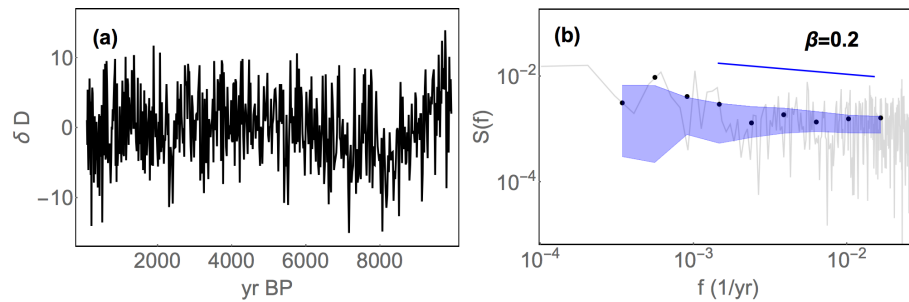


Figure S7. (a): δD anomalies from the Holocene part of the EPICA ice core. (b): Lomb-Scargle periodogram

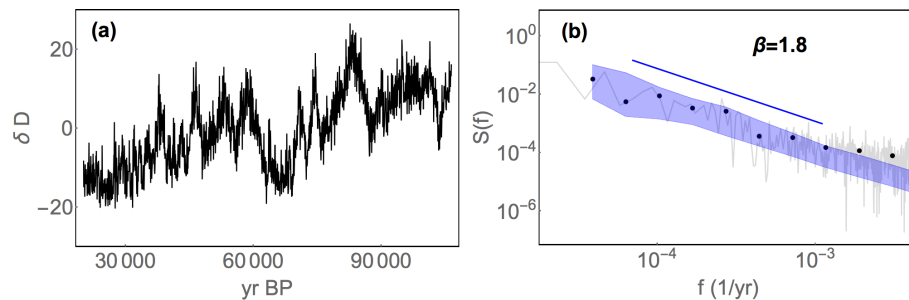


Figure S8. (a): δD anomalies from the last glacial period of the EPICA ice core. (b): Lomb-Scargle periodogram

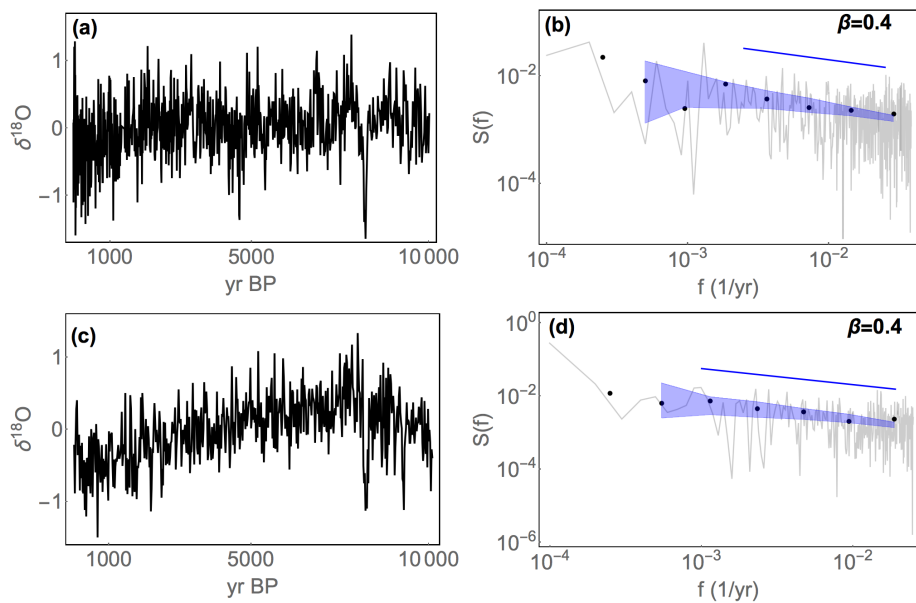


Figure S9. (a): $\delta^{18}\text{O}$ from the Holocene part of the GISP2 ice core. (b): periodogram for the time series in (a). (c) $\delta^{18}\text{O}$ from the Holocene part of the NGRIP ice core. (d): periodogram for the time series in (c). In (b) and (d) the raw periodogram is shown in gray and the log-binned version by black dots. β is estimated from the log-binned periodogram in the region marked by the blue line. The confidence range is shown by the shaded area, estimated from a Monte Carlo ensemble of synthetic fGn with the value of β found from the log-binned periodogram.

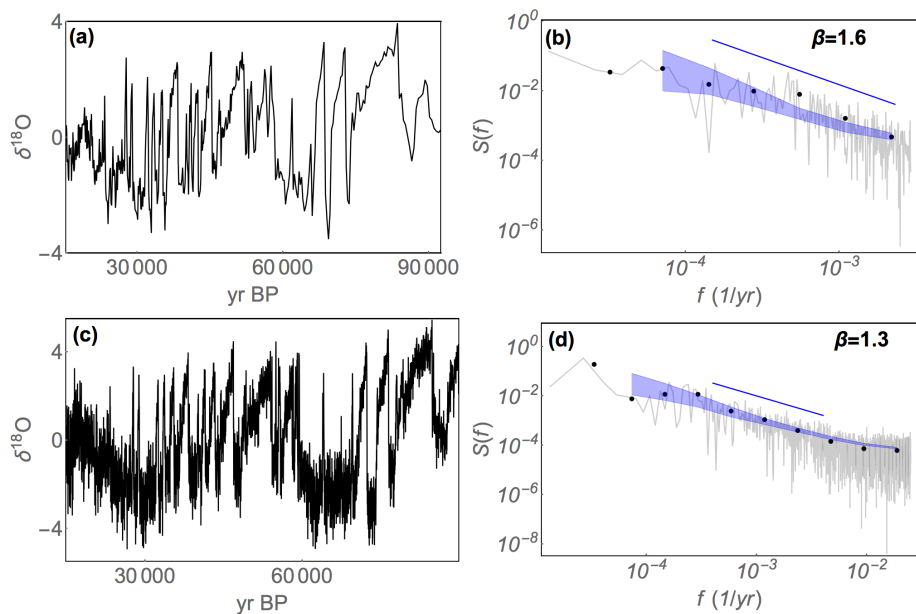


Figure S10. (a): $\delta^{18}\text{O}$ from the last glacial period part of the GISP2 ice core. (b): periodogram for the time series in (a). (c): $\delta^{18}\text{O}$ time series from the last glacial period of the NGRIP ice core. (d): periodogram for the time series in (c).

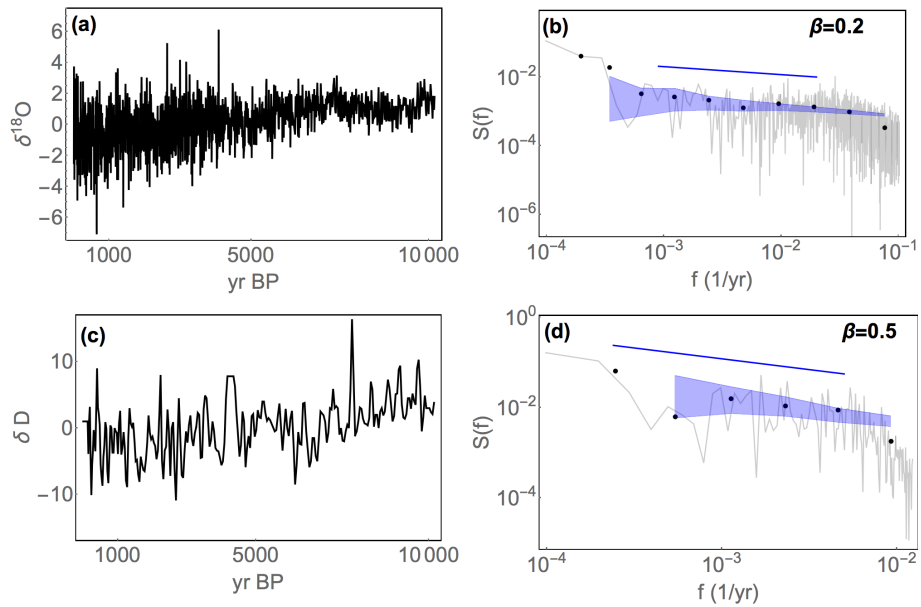


Figure S11. (a): $\delta^{18}\text{O}$ from the Holocene part of the Taylor ice core. (b): periodogram for the time series in (a). (c) δD from the Holocene part of the Vostok ice core. (d): periodogram for the time series in (c).

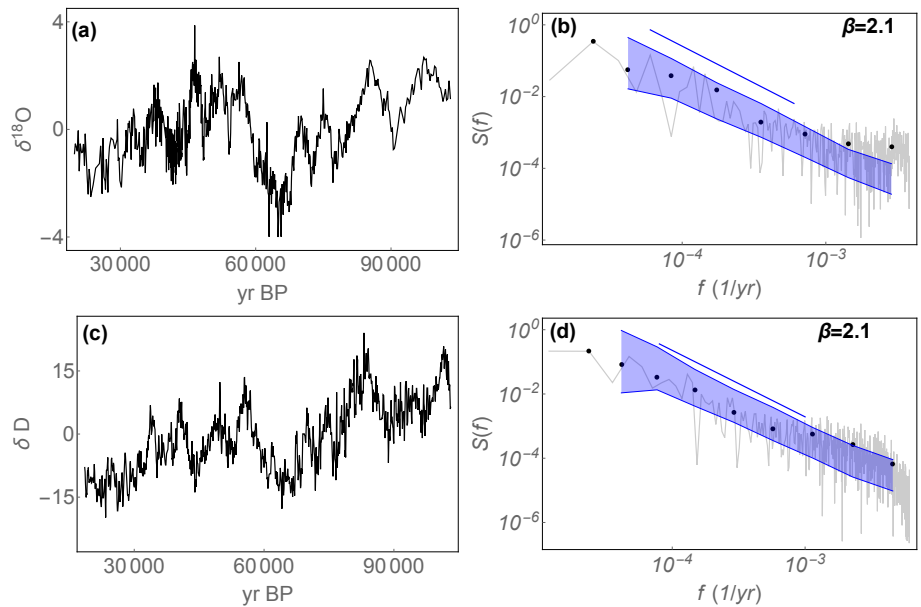


Figure S12. a): $\delta^{18}\text{O}$ from the last glacial period part of the Taylor ice core. (b): periodogram for the time series in (a). (c): δD time series from the last glacial period of the Vostok ice core. (d): periodogram for the time series in (c).